

PAPER • OPEN ACCESS

## Edgewise Structural Damping of a 2.8-MW Land-Based Wind Turbine Rotor Blade

To cite this article: Mayank Chetan and Pietro Bortolotti 2024 *J. Phys.: Conf. Ser.* **2767** 022069

View the [article online](#) for updates and enhancements.

You may also like

- [Degradation of a REBCO conductor due to an axial tensile stress under edgewise bending: a major stress mode of deterioration in a high field REBCO coil's performance](#)  
K Kajita, T Takao, H Maeda et al.
- [Vibration control of floating offshore wind turbines using liquid column dampers](#)  
Zili Zhang and Christian Høeg
- [Edgewise vibration control of wind turbine blades using roller and liquid dampers](#)  
Z L Zhang and S R K Nielsen

**PRIME**  
PACIFIC RIM MEETING  
ON ELECTROCHEMICAL  
AND SOLID STATE SCIENCE

**HONOLULU, HI**  
October 6-11, 2024

*Joint International Meeting of*  
The Electrochemical Society of Japan (ECSJ)  
The Korean Electrochemical Society (KECS)  
The Electrochemical Society (ECS)

Early Registration Deadline:  
**September 3, 2024**

**MAKE YOUR PLANS NOW!**

# Edgewise Structural Damping of a 2.8-MW Land-Based Wind Turbine Rotor Blade

Mayank Chetan<sup>1</sup>, Pietro Bortolotti<sup>1</sup>

<sup>1</sup> National Renewable Energy Laboratory, Golden CO, 80401, USA

E-mail: Mayank.Chetan@nrel.gov

**Abstract.** Modern wind turbines push the predictive capabilities of state-of-the-art aero-servo-elastic tools. The existing limitations hide across the numerical tool chain and can result in serious issues, such as missing aeroelastic instabilities during the design phase. Structural damping is an input that is usually hard to estimate, but also has a major impact on the turbine behavior. In this paper, we discuss an experiment that aims to accurately quantify the structural damping characterizing the edgewise modes of modern wind turbine blades. The experiment is carried out on a 2.8-MW land-based wind turbine and features a fast yaw actuation that induces an edgewise motion on one of the three blades. The Covariant-subspace system identification (Cov-SSI) method is then used to post-process the blade root moment to estimate the short-term edgewise structural damping. Despite limitations of the Cov-SSI method, which consistently under-predicts the absolute values of damping, we observe that structural damping decreases across the first three blade edgewise modes, which is different from the stiffness-proportional damping model that assumes that structural damping increases with the modes. This paper argues that a stiffness-proportional damping model, which is implemented in most aeroelastic tools, is therefore not conservative and might hide aeroelastic instabilities that can instead appear in the field.

## 1 Introduction

The size and flexibility of modern wind turbines challenge the predictive capabilities of state-of-the-art aero-servo-elastic tools. For large turbines, it is important to correctly predict the aeroelastic stability during the design phase [1]. When an instability is missed during design and turbines prove unstable in the field, reliability and safety could become major concerns that may require immediate action, possibly incurring large unplanned financial expenditures. In developing predictive models for highly flexible turbines, structural damping is increasingly one of the most challenging aspects to consider.

To-date, no numerical model can reliably predict structural damping of wind turbine components. Rather, aeroelastic models treat structural damping as an input that must be set by the user, who has to leverage a combination of engineering experience, laboratory testing, and field prototyping to decide the most appropriate values to adopt. To better understand the modal characteristics of wind turbines and their components, designers often rely on natural [2] and forced excitation [3] of the structure. The resulting response is processed using various techniques for operational modal analysis such as stochastic subspace identification (SSI), partial Floquet analysis, and other frequency-based modal identification methods [4, 5]. Ebbehoj et al. [5, 6] compared different methods of computing short-term damping focused on blade edgewise modes for an idling turbine. They concluded that SSI was the most robust approach to analyzing the noisy experimental data. However, it must be highlighted that the SSI method returned much lower values of structural damping in the edgewise direction than anticipated.



This study is part of the Big Adaptive Rotor (BAR) project and the Rotor Aerodynamics, Aeroelastics, and Wake (RAAW) project. BAR supports the design and deployment of the next generation of land-based wind energy technologies, whereas RAAW is a collaboration between the National Renewable Energy Laboratory, Sandia National Laboratories, and the wind turbine manufacturer GE Renewable Energy (GE) to advance the understanding of the dynamic behavior of wind turbines. Both BAR and RAAW are funded by the U.S. Department of Energy's Wind Energy Technologies Office.

During BAR, studies highlighted how wind turbines are increasingly flexible and the margins of aeroelastic stability are getting thinner and thinner [7, 8]. During RAAW, Brown et al. analyzed a numerical model for a highly instrumented 2.8-MW land-based wind turbine and discussed how the characterization of damping is important, especially for the blade edgewise direction [9]. As part of the same experimental campaign, we conducted a series of forced excitation of the same 2.8-MW land-based wind turbine using the yaw actuator. This study is inspired by the work described in Ebbehøj et al. [5] and expands on it by (1) conducting the forced excitation of two blades at two orientations, (2) comparing the results to blade ground testing and numerical models, and (3) focusing on the qualitative aspects of damping trends as a function of blade edgewise modes.

## 2 The Experiment

The land-based GE 2.8-MW prototype wind turbine used in the RAAW experiment has a rotor diameter of 127 m at a hub height of 120 m. The relatively simple experiment involves locking the rotor such that blade 1 (B1) is either in the 12'o clock (blade pointing up) or 6'o clock (blade pointing down) position and is pitched to run (0-degree pitch), whereas the other two blades (B2 & B3) are pitched to feather (90-degree pitch) to reduce the torque loads on the locked rotor. The nacelle is then rotated at the maximum rate about its yaw axis for 8-10 degrees and stopped as quickly as possible. The maneuver generates an excitation in the edgewise direction of B1. After each yaw excitation, the free-decay response of the blades in the edgewise direction is measured using strain gauges located near the root of the blades. Additionally, measurements from various other instruments, such as blade flapwise and tower strain gauges, are collected for further analysis.

Over a 2-month period, we performed the maneuver on blade 1 and blade 3 when the two blades were oriented at either the 12'o clock or 6'o clock position. The yaw-impulse tests were conducted at wind speeds below 5 m/s to reduce the effects of aerodynamic damping on the blades. Figure 1 shows the yaw maneuver and resulting response from the blade root edgewise and tower side-to-side strain gauges.

## 3 Numerical Setup

### 3.1 *OpenFAST Model*

We developed an aero-servo-elastic model of the turbine in the multi-physics framework OpenFAST [10] using detailed aerodynamic and structural properties provided by GE. For the turbine structure we use BeamDyn, a geometrically exact beam model for the blades, and ElastoDyn, a reduced-order Euler Bernoulli beam model, for the tower. The aerodynamics of the blades are modeled using AeroDyn15's steady [10] model with the blade being parameterized with 78 distributed uniformly stations. We verified the OpenFAST model against numerical results from the GE's in-house solvers and validated against experimental results from the blade structural testing and prototype field testing [9]. The match between the models is considered satisfactory, although discrepancies that are greater by approximately 5-40% emerged in the damage equivalent loads of the blade root flapwise moment and tower root fore-aft moment. The blade edgewise quantities also required artificially high values of edgewise structural damping to correctly predict the field measurements.

### 3.2 *Simulations*

Using the validated model, we performed several simulations to test the specifications for the experimental setup and the load envelope for safe operation of the turbine during the yaw-impulse test. The simulations were conducted with a sheared steady inflow at 5 m/s with a power-law shear exponent of 0.18. Figure 1 also shows the yaw maneuver and resulting response from the blade root edgewise and tower side-to-side strain gauges predicted by OpenFAST when B1 is at the 12 o'clock position.

### 3.3 *Mode and Damping Identification*

As a part of the study, we used different system identification methods to evaluate the outputs from the yaw-impulse test. This is a common practice in operational modal analysis [5, 6, 11]. SSI is a system

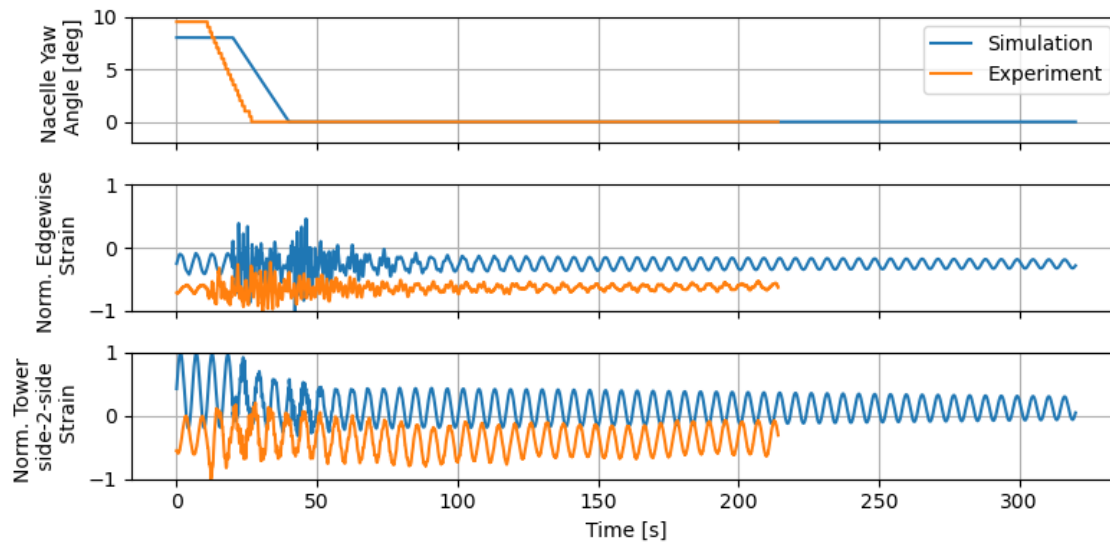


Figure 1: Normalized response of blade (B1) root edgewise and tower side-to-side strain gauges to the yaw-impulse test (simulation and experiment). The offset is due to the normalization of the experiment and simulation done separately to the individual maximums. The test is repeated for both blades (B1 & B3), oriented either pointing up or down, and in both positive and negative yaw directions. A total of 42 individual yaw-impulse tests were performed and recorded.

identification method where the system is expressed as a linear time-invariant  $n$ -degree-of-freedom state-space system under white noise excitation. This can be expressed as [12]:

$$\begin{aligned}x_{k+1} &= Ax_k + w_k \\ y_k &= Cx_k + v_k\end{aligned}$$

Where,  $x_k$  is the discrete-time state vector,  $y_k$  is the measurement output vector,  $A$  is the discrete-state matrix,  $C$  is the discrete output matrix, and  $w_k$  and  $v_k$  represent the effects of unknown inputs.

Our analysis shows that the covariant-based SSI (Cov-SSI) method [13] was the most consistent and stable in providing actionable results. The steps of Cov-SSI involves (i) computing the reduced-order representation using singular value decomposition (SVD), (2) extracting the poles of the identified system, and (3) selecting the stable poles using a stabilization diagram. Once we identify the stable poles, the instantaneous or “short-term” frequency and damping can be calculated. One of the main drawbacks of using this method in the current study is the bias and random error resulting from short time series for each yaw-impulse test. This error is accepted because the focus of the study is on the trend of short-term structural damping across the modes, as opposed to accurately computing the absolute values of structural damping. Ebbehoj [11] tried to overcome this by developing their own method called GP-TARMA, but it needs training data and a representative structural model, thus limiting its applicability for this study.

In this study, we applied the Cov-SSI method on a single strain gauge signal close to the blade root. This is a simplification that in the future might be relaxed if additional strain gauge sensors are available along the span of the blade. Because the rotor is locked in position, each of the tests can be considered as time invariant in nature for using the Cov-SSI method.

## 4 Results

### 4.1 Analysis of Experimental Data

The resulting dataset of 42 individual yaw-impulse tests was processed to identify the first three blade edgewise modes and extract the corresponding short-term damping. Although the tests were repeated as

Table 1: Number of individual yaw-impulse results that were stable enough to compute the corresponding damping using Cov-SSI. The parenthesis show the number of yaw-impulse tests that were conducted for the specific blade and orientation (common across modes) totaling to 42 tests.

Edgewise Mode		Blade Position	
		12 o'clock	6 o'clock
Blade 1 (B1)	First	18 (21)	9 (10)
	Second	18 (21)	10 (10)
	Third	17 (21)	8 (10)
Blade 3 (B3)	First	5 (5)	6 (6)
	Second	5 (5)	5 (6)
	Third	3 (5)	5 (6)

close to the experimental procedure as possible, a few test results did not stabilize sufficiently to extract the modes through the Cov-SSI method. Table 1 shows the number of usable tests for the blades and positions across the first three edgewise modes. The numbers in the parenthesis are the total number of tests in the specific configuration.

Figure 2 shows the distribution of the estimated damping ratio for each individual blade and orientation. The labels on the y-axis are hidden due to proprietary reasons, but all four graphs have the same range. For both blades (B1 and B3), we observe that the estimated damping ratio is similar irrespective of the orientation. This observation creates confidence that the effect of gravity on the edgewise damping for these test is negligible. Next, we observe that blade B1 has an overall higher distribution of damping across modes as compared to B3. There is no known justification to this discrepancy beyond the higher number of yaw-impulse tests that were conducted on B1.

The most important observation in Figure 2 is that the damping ratio across the first three blade edgewise modes for all configurations is similar and trends downward at the higher modes. Ebbelhoj et al. [5] made similar observations with the difference that the damping ratios in that study were constant across the first four blade edgewise modes rather than decreasing. Whether flat or downward, these trends clearly contrast the stiffness-proportional damping used in numerical blade models such as BeamDyn [14].

#### 4.2 Comparison to Structural Laboratory and Numerical Data

Next, we extend the comparison of structural damping by including the measurements obtained by GE during the blade modal test performed in a structural laboratory. The test involved exciting a single blade clamped at the blade root on a stand. The values of structural damping were extracted from accelerometers or strain gauges installed along the blade span. The comparison is presented in Figure 3. The blue bars report the values of structural damping measured during the modal analysis in the laboratory. The laboratory results is limited to the first two edgewise modes. The obvious observation is that the damping for the first two edgewise modes is almost identical. This uniformity strengthens the argument that the stiffness proportional formulation for structural damping might not represent reality.

Figure 3 also includes the values of structural damping predicted by BeamDyn/OpenFAST across modes, shown in orange and green. In the OpenFAST model, users can tune the structural damping to match the structural damping from any one chosen mode per degree of freedom. The structural damping for the subsequent modes is then calculated based on the stiffness-proportional formulation. In this comparison, we first tune structural damping to match the structural damping of the first edgewise mode measured in the structural laboratory. This case is reported with orange bars. Next, we tune structural damping to match the second edgewise mode (reported with green bars). In the orange case, as desired structural damping matches for the first mode, but the higher modes severely overestimate the structural damping, with damping of the third mode exceeding the limit of the y-axis by approximately five times. In the green case, damping in the first mode is underestimated and is set to almost half of the values measured in the structural laboratory, but the structural damping characterizing the third mode is still significantly higher than what was measured in the field. The following four bars, in red, purple, brown, and pink, report the averages from the yaw-impulse test. Similar to what was observed by Ebbelhoj et al. [5], we also note that the values of structural damping extracted from the yaw-impulse test are significantly lower than those measured in the structural laboratory. This systematic under-prediction is verified with the seventh and last set of gray bars, which represent the structural damping predicted

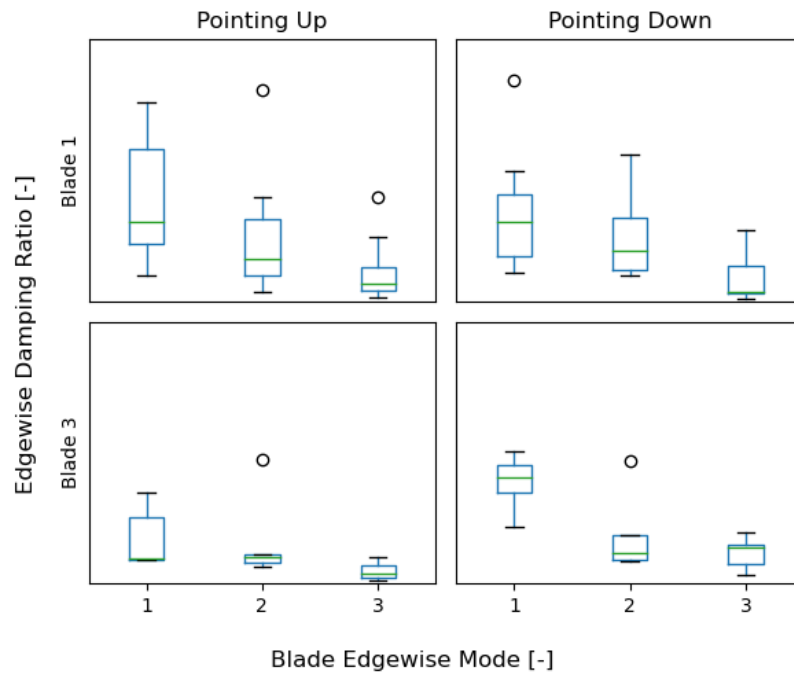


Figure 2: Box plot showing the normalized damping ratio for blade B1 and B3 in the two orientations across the first three edgewise modes. The plot shows the damping ratio calculated for repeated cycles of the yaw-impulse test. The black circles (O) show the outliers. The plot shows that the damping across the first three modes decreases, contradicting conventional beam models that assume a stiffness-proportional formulation for structural damping. The range along the y-axis is masked due to proprietary reasons, but it is constant across the four subplots.

by Cov-SSI when the Cov-SSI approach is applied to the numerical outputs of OpenFAST corresponding to the orange bars. If Cov-SSI was perfect at estimating structural damping, the gray and orange bars would have the same height.

Although the underestimation of the structural damping is a significant drawback of the current study, the upward trend of the gray bars, caused by the stiffness proportional formulation of structural damping in OpenFAST, confirm the ability of the Cov-SSI approach to estimate the trends of structural damping across modes. These results confirm the inadequacy of the stiffness proportional formulation of structural damping, which instead shows flat (laboratory testing [blue]) or downward (Cov-SSI on yaw impulse tests - red, purple, brown, and pink) trends.

## 5 Conclusions and Future Work

This work focuses on understanding the nature of structural damping, which is a key input to accurately predict the dynamic behavior of large and highly flexible wind turbines. Using a validated OpenFAST model of a 2.8-MW land-based prototype wind turbine designed, manufactured, and operated by GE, we excited the edgewise modes of a blade using the yaw system of the turbine. We conducted the experiment at low wind speeds to minimize the impact of aerodynamics. This process was repeated on two blades oriented to point up and point down, for a total of 42 individual data points. The impulse-like response from the blade root edgewise strain gauges was used as input to a Cov-SSI method to estimate the short-term structural damping characterizing the first three blade edgewise modes. The estimated damping ratios show close agreement across the blades and orientations. More importantly, we observe that the damping ratio decreases with the increase in modes. This decrease shows that the stiffness-proportional formulation of structural damping used in BeamDyn and in several other aeroelastic tools is not conservative. The use of non-conservative structural damping models might lead to missing aeroelastic instabilities during the design process. Fixing an aeroelastic instability in the field can incur large costs and cause financial stress to wind turbine manufacturers.

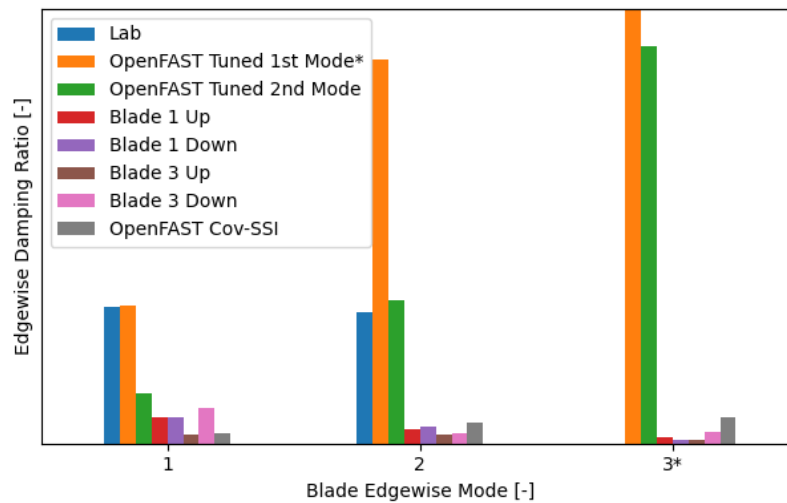


Figure 3: Normalized damping ratio of blade edgewise modes compared across the laboratory experiment, OpenFAST with tuning to edgewise modes 1 and 2 of the laboratory data, and from the various yaw-impulse experiments. For the experimental data, the medians are plotted. \*The damping ratio of OpenFAST tuned to first mode is around five times the upper limit of the y-axis.

The Cov-SSI approach can estimate trends, but greatly underestimates the absolute values of structural damping. This is a weakness that should be better understood and improved. Future work should be dedicated to characterizing the various other sources of damping active in wind turbines, such as structural damping from pitch bearings, the main bearing, yaw bearing, and bolted joints. Additionally, research should investigate the effects of aerodynamic damping on the blades and tower. In the shorter term, formulating structural damping in beam models like BeamDyn should be changed from stiffness proportional to user-defined. The recent changes in the solver Bladed implements Rayleigh damping for each natural mode [15], this approach could be followed to provide a way to tune the damping for the higher modes. At a high level, further work is necessary to continuously improve the predictive capabilities of aeroelastic solvers. Better aeroelastic tools lead to better wind turbines and ultimately, more deployment of wind energy systems.

### Acknowledgment

The authors gratefully acknowledge the technical support of GE Renewable Energy. The research was performed using computational resources sponsored by the U.S. Department of Energy's Office of Energy Efficiency and Renewable Energy and located at the National Renewable Energy Laboratory. This work was authored by the National Renewable Energy Laboratory, operated by Alliance for Sustainable Energy, LLC, for the U.S. Department of Energy (DOE) under Contract No. DE-AC36-08GO28308. Funding provided by the U.S. Department of Energy Office of Energy Efficiency and Renewable Energy, Wind Energy Technologies Office. The views expressed in the article do not necessarily represent the views of the DOE or the U.S. Government. The U.S. Government retains and the publisher, by accepting the article for publication, acknowledges that the U.S. Government retains a nonexclusive, paid-up, irrevocable, worldwide license to publish or reproduce the published form of this work, or allow others to do so, for U.S. Government purposes.

### References

- [1] Volk D M, Kallešøe B S, Johnson S, Pirrung G R, Riva R and Barnaud F 2020 *Journal of Physics: Conference Series* **1618** 052014 ISSN 1742-6596 publisher: IOP Publishing URL <https://dx.doi.org/10.1088/1742-6596/1618/5/052014>
- [2] Carne T G and James G H 2010 *Mechanical Systems and Signal Processing* **24** 1213–1226 ISSN 0888-3270 URL <https://www.sciencedirect.com/science/article/pii/S088832701000097X>

- [3] Osgood R, Bir G, Mutha H, Peeters B, Luczak M and Sablon G 2011 *Structural Dynamics and Renewable Energy, Volume 1* ed Proulx T (New York, NY: Springer) pp 113–124 ISBN 978-1-4419-9716-6
- [4] Jin M, Chen W, Brake M R W and Song H 2020 *Journal of Vibration and Acoustics* **142** ISSN 1048-9002 URL <https://doi.org/10.1115/1.4047416>
- [5] Ebbenhøj K L, Couturier P, Orlowitz E, Høgsberg J and Thomsen J J 2022 *Journal of Physics: Conference Series* **2265** 032043 ISSN 1742-6596 publisher: IOP Publishing URL <https://dx.doi.org/10.1088/1742-6596/2265/3/032043>
- [6] Ebbenhøj K L, Couturier P J, Sørensen L M and Thomsen J J 2023 *Wind Energy Science Discussions* 1–30 publisher: Copernicus GmbH URL <https://wes.copernicus.org/preprints/wes-2023-168/>
- [7] Bortolotti P, Johnson N, Abbas N J, Anderson E, Camarena E and Paquette J 2021 *Wind Energy Science* **6** 1277–1290 ISSN 2366-7443 publisher: Copernicus GmbH URL <https://wes.copernicus.org/articles/6/1277/2021/>
- [8] Bortolotti P, Chetan M, Branlard E, Jonkman J, Platt A, Slaughter D and Rinker J 2024 *Journal of Physics: Conference Series* Publisher: IOP Publishing
- [9] Brown K, Bortolotti P, Branlard E, Chetan M, Dana S, deVelder N, Doubrawa P, Hamilton N, Ivanov C, Jonkman J, Kelley C and Zalkind D 2024 *Wind Energy Science Discussions* 1–28 publisher: Copernicus GmbH URL <https://wes.copernicus.org/preprints/wes-2023-166/>
- [10] 2024 OpenFAST/openfast original-date: 2016-08-31T20:07:10Z URL <https://github.com/OpenFAST/openfast>
- [11] Ebbenhøj K L, Tatsis K, Couturier P, Thomsen J J and Chatzi E 2023 *Mechanical Systems and Signal Processing* **205** 110851 ISSN 0888-3270 URL <https://www.sciencedirect.com/science/article/pii/S0888327023007598>
- [12] Sun S, Yang B, Zhang Q, Wüchner R, Pan L and Zhu H 2023 *Mechanical Systems and Signal Processing* **197** 110326 ISSN 0888-3270 URL <https://www.sciencedirect.com/science/article/pii/S0888327023002339>
- [13] Viberg M 1995 *Automatica* **31** 1835–1851 ISSN 0005-1098 URL <https://www.sciencedirect.com/science/article/pii/0005109895001075>
- [14] Wang Q, Sprague M A, Jonkman J, Johnson N and Jonkman B 2017 *Wind Energy* **20** 1439–1462 ISSN 1099-1824 eprint: <https://onlinelibrary.wiley.com/doi/pdf/10.1002/we.2101> URL <https://onlinelibrary.wiley.com/doi/abs/10.1002/we.2101>
- [15] Collier W 2019 (American Society of Mechanical Engineers Digital Collection) URL <https://dx.doi.org/10.1115/IOWTC2019-7541>